14th International Symposium on Turbulence and Shear Flow Phenomena (TSFP14)
Heidelberg, Germany, July 28–31, 2026

FLOW STRUCTURES IN HINDERED SETTLING OF HEAVY PARTICLES

Simone Tandurella
Complex Fluids and Flows Unit
Okinawa Institute of Science and Technology
Okinawa 904–0495, Japan
simone.tandurella@oist.jp

Alessandro Chiarini
Dipartimento di Scienze e Tecnologie Aerospaziali
Politecnico di Milano
via La Masa 34, 20156 Milano, Italy
alessandro.chiarini@polimi.it

Marco Edoardo Rosti
Complex Fluids and Flows Unit
Okinawa Institute of Science and Technology
Okinawa 904–0495, Japan
marco.rosti@oist.jp

ABSTRACT

The hindered settling of particles in a flow is a ubiquitous phenomenon characterised by a wide span of spatial scales. The main reason behind this is the formation of large particle structures, which have the capacity to activate flow at scales larger than the particles themselves by inducing the formation of shear layers at their collective diffuse interface. The emergence of vertical particle clusters has been previously reported in literature. In this work, we explore new regions of the parameter space, and present findings related to the analysis of particle structures. Notably, in conditions of high-volume fraction and particle-to-fluid density ratio, we observe a regime where the vertical coherence of the flow structures is lost, and a churning condition showing strongly heterogeneous particle distribution sets in. We find additional evidence that this condition has a qualitatively low dependence on Ga.

INTRODUCTION

The settling of heavy particles in a fluid medium is a deep-seated problem of strong scientific and technological interest. Despite sustained efforts in the past century to investigate the physics of such flows, much knowledge, including a phenomenological classification of different regimes, is still missing, even in highly idealised scenarios. This is due to the difficulties of investigating dissipative, long-range interacting, multi-body systems and to the high dimensionality of the parameter space that settling processes inhabit. Even in highly idealised conditions of monodispersion and absence of forcing of the background fluid, at least three non-dimensional parameters are needed to describe the flow conditions: one for the particle concentration, one for their inertia, and one to quantify the intensity of the gravitational pull.

As a result, many investigations have historically focused on the high-dilution, small particle mass limit, which is now generally well understood (Guazzelli & Hinch, 2011). However, outside of these specific conditions, the effects of hindered flow and fluid non-linearity set in, rendering the study of the settling process hard to tackle analytically, numerically and experimentally.

Early theoretical and experimental work by Richardson & Zaki (1954) showed that semi-dilute and dense particle suspensions settling in the Stokes regime experience reduced average settling velocities as a result of the upward volume flux of fluid displaced by the particles. Their study introduced the empirical Richardson–Zaki relation $v_s = v_t(1-\phi)^n$, which expresses the hindered settling velocity of the particle suspension v_s as a function of the single-particle settling velocity v_t and the suspension volume fraction ϕ. The exponent n depends on the Reynolds number based on the particle's terminal velocity, Re_t. Within the Stokes regime, the relation has been found to predict well the settling velocity across a sufficiently wide range of volume fraction. The exact form of the exponent n has been improved through several empirical investigations throughout the years (Garside & Al-Dibouni (1977); Di Felice (1999); Yin & Koch (2007)).

The effect of domain boundaries and the difficulties of imaging the flow especially in dense conditions, have historically strongly affected experimental investigations in the field. Because of this, much of the fundamental study of settling in hindered conditions has resorted to the use of numerical particle-resolved (PR) methods, which consider the particle as a finite-size object, coupled with the flow by the imposition of appropriate two-way momentum flux through its surface. Despite the computational expenditure associated, these methods have provided an approachable avenue for the study of settling in hindered conditions. In this line of works on the subject we find, among others, those of Kajishima & Takiguchi (2002); Uhlmann & Doychev (2014); Willen & Prosperetti (2019); Shajahan & Breugem (2023). The literature on the subject has shown that outside of the Stokes regime, multi-particle structures, or clusters can emerge, due to competing effects on the flow (Fullmer & Hrenya (2017)). Clustering in sedimentation processes can have important impacts, by generating regions of high-speed, downward directed flow which particles sample preferentially, which in some cases may, for example, enhance mean settling rates. In this work, we are interested in expanding the knowledge of the settling of large, semi-dense, assemblies of heavy particles. Compared to most previous studies, we aim to explore a region of the parameter space characterised by higher particle mass loading, in terms of both particle concentration and inertia. In this limit, particles are generally expected to be less influenced by the fluid, and collisional effects to become relevant. In the following, we present results connected with clustering of the particles.

METHODS

In this work, we aim to elucidate the reciprocal interaction of the emerging many-particle clusters with the different scales of the flow, the properties of the flow as a result of the forcing imposed by the particles, and the influence on particle settling dynamics. To do this, we investigate a PR-DNS numerical setup consisting in $O(10^4–10^5)$ spherical, monodisperse, heavy particles of diameter d falling in a $L_x \times L_y \times L_z = 80d \times 80d \times 200d$ triperiodic domain. A vertically-aligned acceleration g is imposed to simulate the effect of settling, along with a fixed pressure gradient. To compute the fluid motion we solve the incompressible Navier-Stokes equations in a finite-difference solver employing a second-order central finite difference scheme in space and Adams-Bashforth in time. The incompressibility constraint is enforced using a fractional step method. The particle motion is computed according to the Newton-Euler equations, and coupled to the fluid through the Eulerian Immersed Boundary Method developed by Hori *et al.* (2022). Particle-particle interactions are computed using a soft-sphere collision model, while lubrication forces arise implicitly from the IBM. In line with recent literature, we use as non-dimensional groups the volume fraction ϕ, the particle-to-fluid density ratio γ, and the Galileo number Ga:

$$\phi = \frac{n_p V_p}{V}, \qquad \gamma = \frac{\rho_p}{\rho_f}, \qquad Ga = \frac{\sqrt{(\gamma-1)gd^3}}{\nu} \tag{1}$$

Here, n_p is the number of particles, V_p is the volume of a single particle, V is the total volume in the domain, ρ_p and ρ_f are the densities of the particles and fluid respectively, and ν is the kinematic viscosity. Based on these non-dimensional quantities, we perform a total of nine main simulations, spanning about a decade in each parameter. Three different mass loadings are investigated, with three values of Ga each. The exact values used are reported in table 1.

Table 1. Non-dimensional parameters and resolution for the main simulation sets. N is the number of grid points in each cartesian direction. Entries are arranged in order of increasing mass loading: low (L), medium (M), high (H).

ID	ϕ	γ	Ga	$N_x \times N_y \times N_z$
● L1	0.01	10	61	$960 \times 960 \times 2400$
● L2	0.01	10	182	$960 \times 960 \times 2400$
● L3	0.01	10	545	$1280 \times 1280 \times 3200$
● M1	0.01	100	61	$960 \times 960 \times 2400$
● M2	0.01	100	182	$960 \times 960 \times 2400$
● M3	0.01	100	545	$1280 \times 1280 \times 3200$
● H1	0.10	100	61	$960 \times 960 \times 2400$
● H2	0.10	100	182	$960 \times 960 \times 2400$
● H3	0.10	100	545	$1280 \times 1280 \times 3200$

RESULTS

An initial qualitative analysis of the results reveals large phenomenological differences across the cases tested. We illustrate the variety in flow structures by showing in fig. 1 the fluid vertical velocity field $u_z(\boldsymbol{x})$ for each case. For the lowest mass loading case, we find multiple domain-spanning elongated structures, which appear to curve or branch. As density ratio increases (middle mass loading case), we find strongly vertical structures, spanning the entirety of domain width, and showing very strong vertical fluid correlation. This result is expected as particle inertia increases the scale of flow fluctuations sampled by the particles. Finally, a further increase of mass loading through an increase in volume fraction appears to induce a transition in the flow: the vertical structures lose the coherence that characterized the previous state and a churning, chaotic condition takes their place. Within the investigated parameter range, we find that influence of Ga on the overall flow structures to be relatively minor compared to the other two parameters, affecting mostly the vertical velocity in terms of magnitude.

The presence of a chaotic state in the fluid naturally leads to question of particle distribution in the flow. In order to give an initial answer to this, we investigate the Voronoi volumes distribution (Monchaux *et al.* (2010)) as a measure of particle clustering. The Voronoi polyhedron associated with the a particle consists in all the points within the domain that are closest to that particle than any other. The volume of the Voronoi polyhedron of the i-th particle is indicated by V_v^i and is termed, for simplicity, the Voronoi volume. The smaller V_v^i, the closer the particle is to others, and thus the more clustered. The results of the volumes distribution are presented in fig. 2. To gauge the degree of clustering, we compare against the typical distribution of volumes obtained for a non-overlapping, uniformly random (NUR) distributed suspension of spheres with the same volume fraction as that investigated. Since $\sum_i V_v^i = V$, the presence of small volumes is always accompanied by larger ones, associated with particles near void regions. For unimodal distributions, there are two values of V_v where the intersection of the distributions with the *NUR* reference occurs. These are often used to assess whether particles belong to the clusters, void regions or neither.

In the lowest mass loading case we observe a clear effect of Ga: for the lowest values $Ga = 61$ we observe a distribution presenting fewer extreme volumes, and a stronger central peak, which suggests a stabilisation effect over the suspension, especially at short ranges. For higher values of Ga this stabilisation effect appears to be either lost or subdominant compared to other effects, as the distributions widen and the peaks gradually shift to smaller values of volume. By comparison, for the middle mass loading cases a distribution much closer to that of the reference random case is observed, despite there not being a complete overlap. This may indicate relatively low amounts of clustering, especially when compared to the previous cases. For this middle mass loading case, variation of Ga within the range investigated appears to play a minor role. Finally, for the highest mass loading cases we obtain a broad distribution, where the resolved portion of the tail ends show a volume ratio of up to 2–10 times that of the reference distribution for the same probability values. This highlights the presence of highly clustered and empty regions. Again, we do not observe strong differences across values of Ga.

While the Voronoi volume offers a first quantitative measure about the levels of clustering in the suspension, it does not

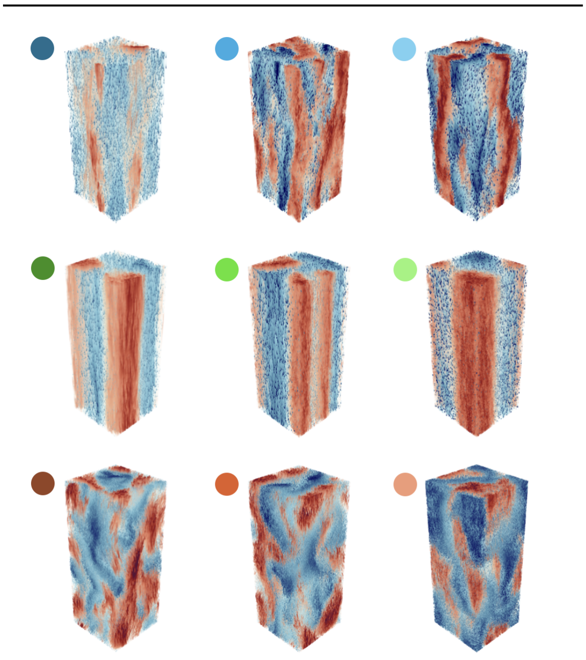

Figure 1. Snapshots of the instant vertical velocity field for the simulations reported in table 1. Red (blue) colouring corresponds to regions of upward (downward) directed fluid motion. The average fluid velocity is set to 0 within the domain.

answer questions about the microstructure, and in particular to its directional dependence. We look into more detail about the particle microstructure within the flow, by measuring the pair distribution function $g(\boldsymbol{r})$:

$$g(\boldsymbol{r}) = \frac{1}{n_p(n_p-1)} \sum_{j=0}^{n_p} \sum_{\substack{i=0,\\ i\neq j}}^{n_p} \delta((\boldsymbol{x}_j - \boldsymbol{x}_i) - \boldsymbol{r}) \tag{2}$$

Where $\boldsymbol{x}_i$ is the location of the i-th particle's centre and δ is the Dirac delta. Due to the cylindrical symmetry of the problem, the domain of g reduces to a radial and a vertical component. That is, in the present case $g(\boldsymbol{r}) = g(r_\parallel, r_\perp)$. We are interested in comparing the pair distribution function to the base random case in order to separate dynamic effects from geometrical ones. Because of this, we study the deviation of the pair distribution function from the reference random case: $g^*(r_\parallel, r_\perp) = g(r_\parallel, r_\perp) - g_{NUR}(r_\parallel, r_\perp)$, shown in fig. 3. In the case of the highest mass loading, the pair distribution anomaly shows strong symmetry in the polar plane for all values of Ga, suggesting a microstructure lacking strong directional preference. For the intermediate mass loading cases, we observe a small positive correlation across the entire region considered. A region of stronger positive correlation is found in the horizontal direction closest to the particle, while in the vertical direction (i.e. in the particle wake) a very narrow peak of particle concentration at contact is observed, surrounded by a relative deficit of particles compared to the rest of the region considered. For $Ga = 61$ the pair distribution anomaly becomes negative in this region, extending for approximately $5d$ in the wake. A narrow region of particle deficit is present also in the horizontal direction, while the region of positive correlation is still present, but shifted towards higher values of $r_\parallel$. This directional preference of particle spatial correlation

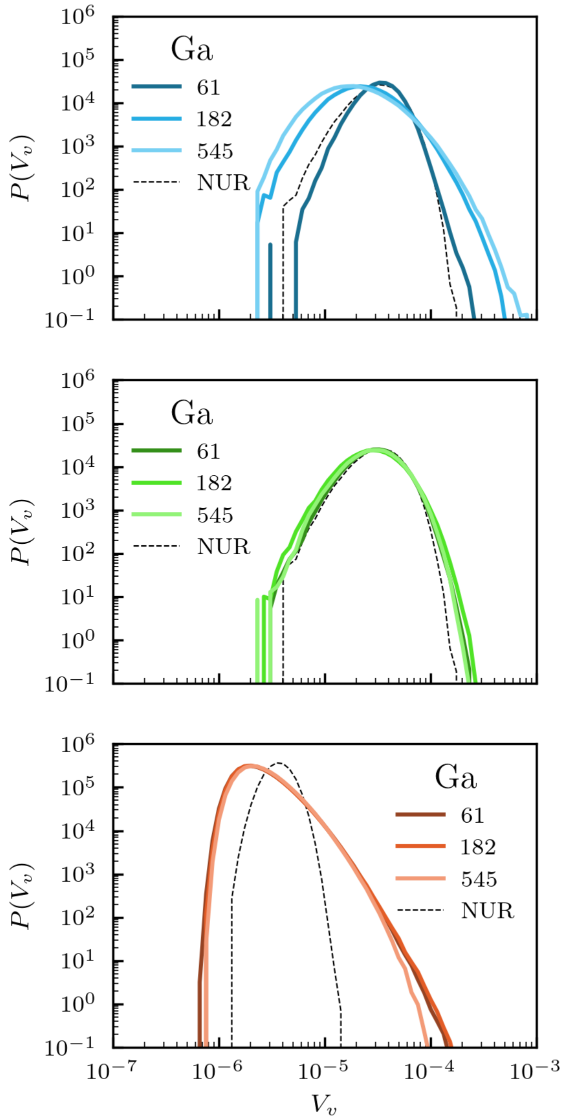

Figure 2. Voronoi volumes distribution for the cases investigated. The wider the Voronoi distribution, the higher the degree of clustering. The line indicated as NUR is for the non-overlapping, uniformly random particle distribution, which is dependent on ϕ.

may support the idea of a statistical effect also over the shape of the Voronoi polyhedra and may affect conclusions over the degree of clustering that may be derived solely from the volumes distribution. For the lowest volume fraction we observe stronger variation across values of Ga. For $Ga = 61$ the pair distribution anomaly is strongly negative in the immediate surroundings, in both the axial and radial directions. In the axial direction, the wake deficit extends up to approximately $10d$. Particle concentration higher than reference is present in the radial direction past approximately $2d$, similarly to the corresponding intermediate mass loading case. This appears consistent with the suspension regularisation effects observed from the Voronoi analysis. The $Ga = 182$ and 545 cases in comparison see the emergence of strong, vertically elongated clusters. For the $Ga = 182$ clustering is especially strong in the wake, in the immediate radial direction and at contact; a region of relative particle deficit however appears in a region around in the particle vicinity at an angle of 45–60° from the $r_\parallel$ axis.

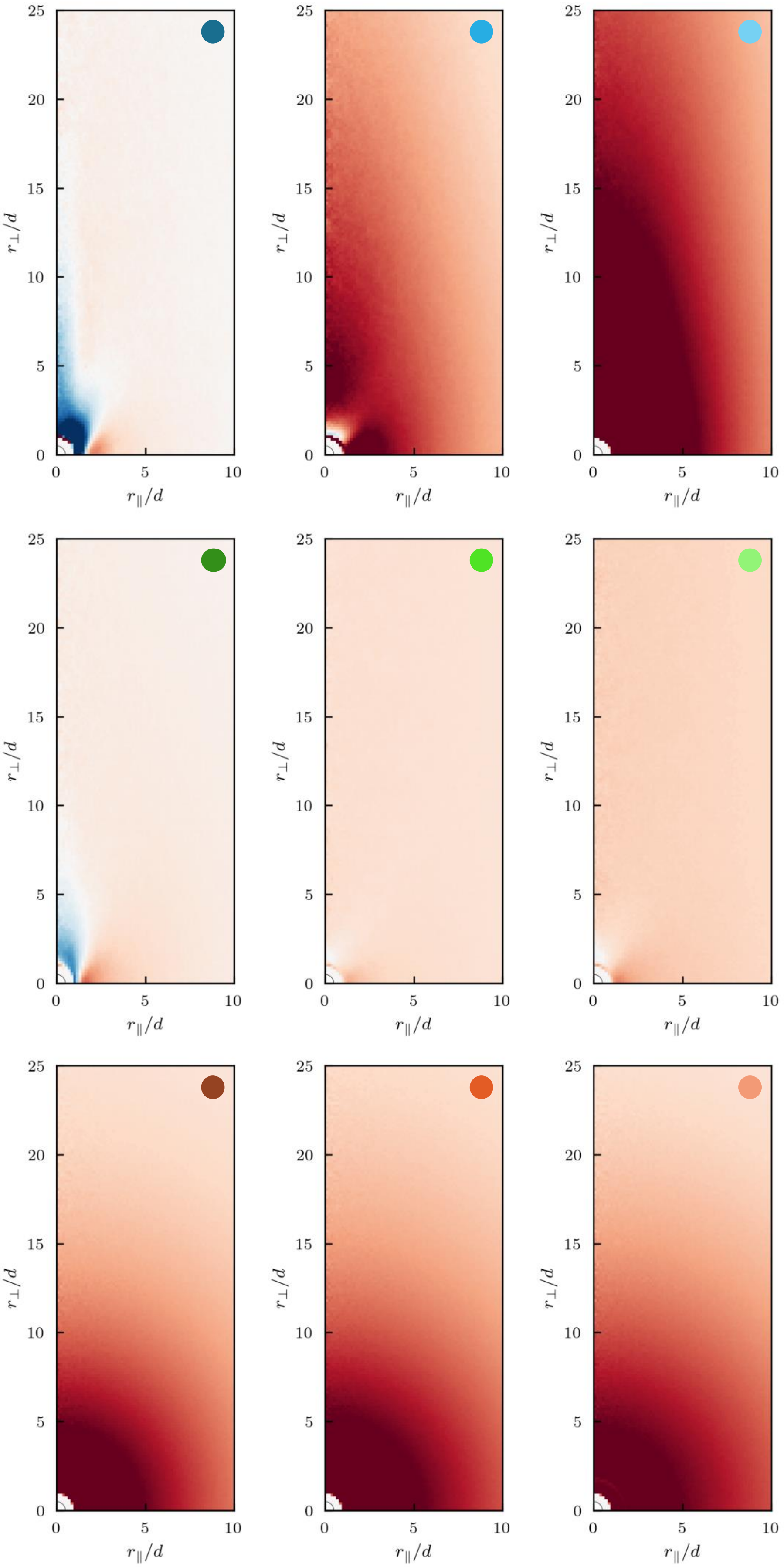

Figure 3. Pair distribution function anomaly (i.e. $g^*(r_\parallel, r_\perp) = g(r_\parallel, r_\perp) - g(r_\parallel, r_\perp)_{NUR}$ for the cases investigated. *Ga* increases from left to right, while mass loading increases from top to bottom.

CONCLUSIONS

As a whole, our preliminary results present a complex picture and show richly heterogeneous behaviour within the parameter space investigated. In the lightest mass loading case, we observe a comparatively large influence of the fluid. This is expected, considering the lower ρ_p/ρ_f. As a result, particles appear be more strongly affected by hydrodynamic effects, with the pair distribution function showing strong dependence on *Ga*. We observe the presence of strongly anisotropic clusters, similar, to some extent, to the ones observed by Uhlmann & Doychev (2014). In our case, however, the vertical correlation appears to weaken, and not span the full domain. This can be appreciated as well from the vertical velocity structures of fig. 1. The middle mass loading case, instead, shows strong vertical correlation in the fluid. However, the fluid correlation does not appear to extend to the particles, with the Voronoi volumes appearing randomly distributed, and g^* showing weak clustering. Only for low *Ga* hydrodynamic wake screening effects appear to remain relevant, despite the high density ratio. This dynamic, which occurs also for the low mass loading case, seems coherent with the the theoretical basis of the screening effect (Koch & Shaqfeh (1991)). In the high-volume fraction limit, we observe a radical transition in the overall dynamics. Firstly, vertical coherence is lost both in the fluid and in the particle structures. Despite the same ρ_p/ρ_f as the middle mass-loading case, the wake screening mechanism found in the low *Ga* case appears thwarted. Secondly, strong clustering, independent of *Ga* sets in. For the high *Ga* cases, the present results may suggest a switch in the mechanism behind clustering. Overall, the results presented help in clarifying our currently still incomplete understanding of settling in hindered, inertial conditions.

REFERENCES

Di Felice, R 1999 The sedimentation velocity of dilute suspensions of nearly monosized spheres. *International Journal of Multiphase Flow* **25** (4), 559–574.

Fullmer, William D. & Hrenya, Christine M. 2017 The Clustering Instability in Rapid Granular and Gas-Solid Flows. *Annual Review of Fluid Mechanics* **49** (1), 485–510.

Garside, John & Al-Dibouni, Maan R. 1977 Velocity-Voidage Relationships for Fluidization and Sedimentation in Solid-Liquid Systems. *Industrial & Engineering Chemistry Process Design and Development* **16** (2), 206–214.

Guazzelli, Élisabeth & Hinch, John 2011 Fluctuations and Instability in Sedimentation. *Annual Review of Fluid Mechanics* **43** (Volume 43, 2011), 97–116.

Hori, Naoki, Rosti, Marco E. & Takagi, Shu 2022 An Eulerian-based immersed boundary method for particle suspensions with implicit lubrication model. *Computers & Fluids* **236**, 105278.

Kajishima, Takeo & Takiguchi, Saotshi 2002 Interaction between particle clusters and particle-induced turbulence. *International Journal of Heat and Fluid Flow* **23** (5), 639–646.

Koch, Donald L. & Shaqfeh, E. S. G. 1991 Screening in sedimenting suspensions. *Journal of Fluid Mechanics* **224**, 275–303.

Monchaux, R., Bourgoin, M. & Cartellier, A. 2010 Preferential concentration of heavy particles: A Voronoï analysis. *Physics of Fluids* **22** (10), 103304.

Richardson, J. F. & Zaki, W. N. 1954 The sedimentation of a suspension of uniform spheres under conditions of viscous flow. *Chemical Engineering Science* **3** (2), 65–73.

Shajahan, Tariq & Breugem, Wim-Paul 2023 Inertial effects in sedimenting suspensions of solid spheres in a liquid. *International Journal of Multiphase Flow* **166**, 104498.

Uhlmann, Markus & Doychev, Todor 2014 Sedimentation of a dilute suspension of rigid spheres at intermediate Galileo numbers: The effect of clustering upon the particle motion. *Journal of Fluid Mechanics* **752**, 310–348.

Willen, Daniel P. & Prosperetti, Andrea 2019 Resolved simulations of sedimenting suspensions of spheres. *Physical Review Fluids* **4** (1), 014304.

Yin, Xiaolong & Koch, Donald L. 2007 Hindered settling velocity and microstructure in suspensions of solid spheres with moderate Reynolds numbers. *Physics of Fluids* **19** (9), 093302.